Kinetics of the Reactions of N(^{4}S) Atoms with O_2 and CO_2 over Wide Temperatures Ranges

Abel Fernandez, A. Goumri, and Arthur Fontijn*

High-Temperature Reaction Kinetics Laboratory, The Isermann Department of Chemical Engineering, Rensselaer Polytechnic Institute, Troy, New York 12180-3590

Received: July 21, 1997; In Final Form: October 21, 1997[⊗]

Rate coefficients for the depletion of ground-state nitrogen atoms by O_2 have been measured using a high-temperature photochemistry reactor. The N atoms were generated by VUV flash photolysis of N_2O, and the relative concentrations were monitored by resonance fluorescence. The data are best fitted by the expression $k(400-1220\ \mathrm{K}) = 2.0 \times 10^{-18}(T/\mathrm{K})^{2.15} \exp(-2557\ \mathrm{K}/T)\ \mathrm{cm^3\ molecule^{-1}\ s^{-1}}$ with 2σ precision limits varying from ±7% to ±20% depending upon temperature, and corresponding 2σ accuracy limits of ±23% to ±30%. Good agreement is found with earlier, electrical discharge initiated, rate coefficient measurements for the 280−910 K domain. Semiempirical theory-based calculations are presented that lead to a plot nearly indistinguishable from those of the present results and the Baulch et al. recommendation for the 300−5000 K temperature range. These yield a classical barrier $E_0^{\ddagger}$ of 27.4 kJ mol^{-1}. No reaction with CO_2 could be observed; upper limit rate coefficients were obtained from 285 to 1140 K. These upper limits indicate that the reverse reaction is insignificant for models of nitrate ester and nitramine propellant dark zones.

Introduction

Models of the combustion of nitrate ester and nitramine propellants, especially those for the dark zone structures, depend critically on rate coefficients for[1]

$$\mathrm{NO(X^2\Pi) + CO(X^1\Sigma) \rightarrow N(^4S) + CO_2(X^1\Sigma)} \qquad \Delta H^0_{298} = 99.4\ \mathrm{kJ\ mol^{-1}}\ \text{(ref 2)} \quad (1)$$

which are uncertain. This spin-forbidden reaction is not readily amenable to direct observation, but its reverse

$$\mathrm{N(^4S) + CO_2(X^1\Sigma) \rightarrow NO(X^2\Pi) + CO(X^1\Sigma)} \qquad \Delta H^0_{298} = -99.4\ \mathrm{kJ\ mol^{-1}}\ \text{(ref 2)} \quad (2)$$

has been studied several times. Avramenko and Krasnen'kov[3] performed a flow tube experiment and obtained an expression $k(291-523\ \mathrm{K}) = 3.2 \times 10^{-13} \exp(-1711\ \mathrm{K}/T)\ \mathrm{cm^3\ molecule^{-1}\ s^{-1}}$. Later flow tube investigators showed those observations to be due to N-atom recombination with CO_2 as the third body.[4,5] Upper limits for reaction 2 have been reported by Rawlins and Kaufman[4] and Herron and Huie[6] of, respectively, $k_2(300\ \mathrm{K}) < 10^{-19}$ and $k_2(560\ \mathrm{K}) < 2 \times 10^{-16}\ \mathrm{cm^3\ molecule^{-1}\ s^{-1}}$. Since then, modeling of the results of a shock tube study of C_2N_2/CO_2/Ar mixtures[7] yielded as a byproduct $k_2(2510-3510\ \mathrm{K}) = 1.4 \times 10^{-12} \exp(-1114\ \mathrm{K}/T)\ \mathrm{cm^3\ molecule^{-1}\ s^{-1}}$. This expression would indicate a readily measurable reaction at room temperature. While such modeling of a secondary reaction is uncertain and extrapolation over such a large temperature range would be a doubtful procedure, their result[7] when applied to dark zones (temperatures ≈1200−1500 K) would suggest that reaction 1 is the major radical source.[1] We therefore decided to reinvestigate reaction 2 with an isolated elementary reaction technique, high-temperature photochemistry (HTP), which allowed observations on this reaction up to dark zone temperatures.

In addition, the extensively measured reaction

$$\mathrm{N(^4S) + O_2(X^3\Sigma) \rightarrow NO(X^2\Pi) + O(^3P)} \qquad \Delta H^0_{298} = -133\ \mathrm{kJ\ mol^{-1}}\ \text{(ref 2)} \quad (3)$$

which is a step in the Zeldovich NO formation mechanism,[8] was studied, partially as a check on the experimental method. Previously, rate coefficients of reaction 3 have been measured in isolation by electrical discharge techniques: from 280 to 326 K in a low-pressure sphere[9,10] and from 300 to 910 K in tubular fast-flow reactors.[10−13] The present work, in which the pseudo-static HTP technique was used, extends the temperature domain and yields a semiempirical value for the classical barrier.

Technique

The experiments were performed in the HTP reactor, described previously by Ko et al.[14] The apparatus was operated in the VUV flash photolysis−resonance fluorescence (FP−RF) mode. Nitrogen atoms were produced by photolyzing N_2O.[15] The flash lamp[16] operated on approximately 150 mbar of N_2 and was supplied with a MgF_2 ($\lambda > 110$ nm) window. The 120 nm N-atom resonance radiation, produced by a microwave discharge flow lamp using 1−3 mbar of He, passed through a 10.5 cm long cell through which flowed 0.53% N_2O in Ar. The use of N_2O as a light filter was suggested by the work of Husain and Slater.[17] N_2O attenuates the O-atom resonance radiation at 130 nm 24 times as much as the N-atom resonance radiation.[15] The filter was optimized by producing O atoms in the reactor by flash photolysis of SO_2 and increasing the N_2O partial pressure to 0.32 mbar, at which point the O-atom resonance fluorescence[18] appeared completely attenuated. The fluorescence radiation passed through a MgF_2 window before being detected by a solar-blind photomultiplier tube.

Lee et al.[19] have used a somewhat similar FP−RF apparatus for N-atom studies in the 230−400 K domain. They used N_2O at partial pressures from 0.16 to 0.53 mbar and estimated [N]

[⊗] Abstract published in *Advance ACS Abstracts,* December 1, 1997.

S1089-5639(97)02365-7 CCC: $15.00
Published on Web 01/01/1998

TABLE 1: Summary of Rate Coefficient Measurements on the N + O_2 → NO + O Reaction

T,[a] K	*P*, mbar	[M], 10^{18} cm^{-3}	[N_2O],[b] 10^{15} cm^{-3}	*F*,[c] J	$[O_2]_{max}$, 10^{15} cm^{-3}	*z*,[d] cm	$\bar{v}$, cm s^{-1}	$k \pm \sigma_k$, 10^{-15} cm^3 molecule^{-1} s^{-1}
404	133	2.39	6.35	116	29.3[e]	7.0	4.3	1.44 ± 0.17
417	133	2.32	3.01	116	23.8[e]	7.0	8.9	2.07 ± 0.02
455	266	4.25	5.60	116	18.1[e]	7.0	4.9	4.07 ± 0.28
456	133	2.12	2.80	116	13.4[e]	7.0	9.8	2.38 ± 0.34
476	133	2.03	2.68	59	13.4[e]	7.0	10.3	3.83 ± 0.21
535	133	1.81	4.82	118	4.4[f]	19.5	5.7	13.7 ± 0.8
551	133	1.75	2.35	116	1.61[f]	7.0	11.7	19.8 ± 0.7
558	133	1.73	4.60	116	3.14[f]	7.0	6.0	17.8 ± 0.8
562	133	1.72	2.30	59	1.37[f]	7.0	11.9	17.5 ± 0.6
615	133	1.57	2.07	116	6.70[e]	7.0	13.3	31.0 ± 0.8
653	266	2.96	3.96	116	1.82[f]	7.0	7.0	45.2 ± 3.1
671	133	1.44	3.80	116	2.79[f]	7.0	7.2	47.8 ± 0.2
724	133	1.33	1.80	59	0.90[f]	7.0	15.4	86.1 ± 1.2
731	266	2.64	3.54	116	1.63[f]	7.0	7.8	88.8 ± 1.8
736	133	1.31	1.76	116	0.30[g]	7.0	15.6	110 ± 24
770	133	1.25	1.68	116	0.16[g]	7.0	16.3	151 ± 44
775	133	1.25	3.32	116	0.70[g]	7.0	8.3	113 ± 10
800	266	2.42	3.24	116	0.32[g]	7.0	8.5	108 ± 9.2
811	133	1.19	1.60	59	0.10[g]	7.0	17.2	186 ± 17
812	133	1.19	3.17	116	0.31[g]	7.0	8.7	165 ± 33
901	133	1.07	1.44	116	0.11[g]	7.0	19.1	233 ± 54
915	133	1.06	2.82	59	0.16[g]	7.0	9.8	252 ± 17
932	133	1.04	1.39	43	0.95[g]	7.0	19.8	283 ± 37
935	266	2.07	2.77	30	1.30[f]	7.0	9.9	286 ± 17
936	133	1.03	1.39	30	0.64[f]	7.0	19.9	219 ± 28
995	266	1.94	2.60	116	0.15[g]	7.0	10.6	474 ± 34
1009	133	0.96	1.29	59	0.14[h]	3.5	21.4	483 ± 45
1024	133	0.94	2.52	116	0.16[g]	7.0	10.9	722 ± 89
1031	189	1.33	3.23	142	0.28[h]	4.5	8.5	391 ± 52
1077	133	0.90	1.20	116	0.09[g]	7.0	22.9	691 ± 130
1126	133	0.86	1.15	116	0.09[g]	7.0	23.9	1004 ± 17
1129	266	1.71	2.29	72	0.25[g]	7.0	11.9	828 ± 108
1131	133	0.85	1.15	72	0.07[g]	7.0	24.0	752 ± 157
1132	133	0.85	1.15	59	0.04[g]	7.0	24.0	957 ± 555
1144	133	0.84	1.13	74	0.07[g]	7.0	24.3	953 ± 227
1187	133	0.81	1.09	116	0.07[g]	7.0	25.2	874 ± 170
1221	133	0.79	1.06	85	0.07[h]	3.5	25.9	851 ± 27

[a] $\sigma_T/T = 2\%$. [b] Photolyte. [c] Flash energy. [d] Distance from cooled inlet to reaction zone. [e] Used pure O_2. [f] Used 5% O_2 in Ar. [g] Used 0.53% O_2 in Ar. [h] Used 0.50% O_2 in Ar.

< 10^{11} cm^{-3}. To keep [N] as low as possible, N_2O pressures somewhat smaller were used in the present work, Table 1. This resulted in S/N ≈5−10 and a signal-to-background ratio ≈2−3. The reason for keeping [N] low in the present work is to prevent interference from N-atom recombination and from the fast reaction[19,20]

$$N(^4S) + NO(X^2\Sigma) \rightarrow N_2(X^1\Sigma) + O(^3P) \qquad (4)$$

NO forms as a result of the photolysis; it is also a product of reaction 3.

The experiments were carried out under pseudo-first-order conditions, [N] ≪ [O_2] ≪ [N_2] and [N] ≪ [CO_2] ≪ [N_2]. N_2 was used as the bath gas since it rapidly quenches excited N atoms, N(^{2}D), and N(^{2}P), produced by the photolysis.[19] The fluorescence intensity *I*, proportional to [N], can be written as

$$I = I_0 \exp(-k_{ps1}t) + B \qquad (5)$$

where I_0 is the intensity at time $t = 0$, k_{ps1} is the pseudo-first-order rate coefficient, and *B* is the background due to scattered light. The values of k_{ps1} were obtained by fitting[21] the observed *I* vs *t* profiles to eq 5. A two-stage residual analysis[22] was used to verify the exponentiality of the *I* vs *t* plots. Typically five or six k_{ps1} values with [O_2] or [CO_2] varying by about a factor of 10 were used to obtain rate coefficients at the temperature and pressure of the experiment, Figure 1.

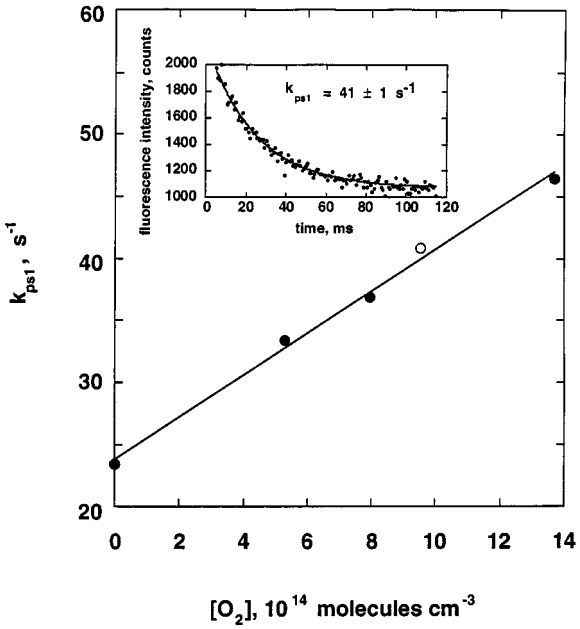

Figure 1. Plot of a pseudo-first-order decay of relative [N] versus [O_2], obtained at 561 K. The inset corresponds to the open circle and shows the decrease of fluorescence intensity with respect to time.

N_2 bath gas, from liquefied N_2 of 99.995% purity, was supplied by Praxair. He (99.999% UHP), used in the flow lamp, N_2O (99.99% UHP), used as the photolyte, 0.53% N_2O

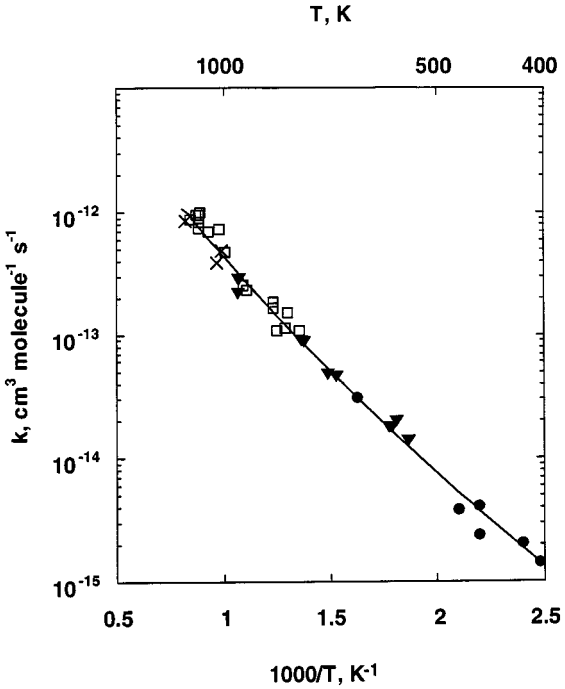

Figure 2. Summary of the N + O_2 → NO + O rate coefficient measurements: ●, measurement using pure O_2; ▼, measurement using 5% O_2; □, measurement using 0.53% O_2; ×, measurement using 0.50% O_2; —, best fit to the measurements, eq 6.

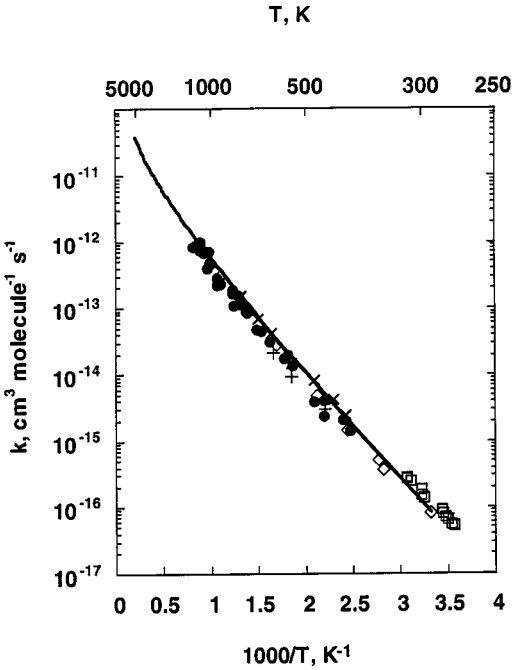

Figure 3. Comparison of the rate coefficient measurements of the N + O_2 → NO + O reaction with other data: ●, present study, 400−1220 K; □, Becker et al.,[9,10] 280−326 K; ◇, Wilson,[10,11] 300−910 K; +, Vlastaras and Winkler,[10,12] 455−605 K; ×, Clyne and Thrush,[10,13] 410−755 K; —, Baulch et al. recommendation,[20] eq 7, 300−5000 K.

(99.995% in Ar (99.998%)), used in the N_2O filter, O_2 (99.98% UHP), 0.53% O_2 (99.999% UHP in Ar (99.999% UHP)), 0.50% O_2 (99.6% Extra Dry in Ar (99.998% Prepurified)), and CO_2 (99.8% Bone Dry) were obtained from Matheson. Five percent O_2 (99.996% in Ar (99.998%)) was obtained from Scott Specialty Gases.

Results and Discussion

N + O_2. The measurements spanned the 404−1221 K temperature domain. The upper limit arose from the thermal instability of the photolyte, N_2O, and the lower limit from the slowness of the reaction. The data may be seen from Table 1 to be independent of the total pressure, P, and the corresponding total gas concentration, [M], the average gas velocity, $\bar{v}$, the distance from the tip of the cooled inlet to the reaction zone, *z*, the flash lamp energy, *F*, and the N_2O concentration. The data are also independent of the stock oxygen gas used. The four different oxygen cylinders used each had different concentrations and were purchased at different times to guard against the presence of accidental impurities. The data are plotted in Figure 2 and show a slightly curved Arrhenius plot. A nonlinear least-squares fit,[23] to the format $k(T) = AT^n \exp(-E/RT)$, weighted according to the uncertainties of the rate coefficients and the temperatures, as indicated in Table 1, yields

$$k_3(400-1220\ \mathrm{K}) = 2.0 \times 10^{-18}(T/\mathrm{K})^{2.15} \exp(-2557\ \mathrm{K}/T)\ \mathrm{cm}^3\ \mathrm{molecule}^{-1}\ \mathrm{s}^{-1} \quad (6)$$

The variances and covariances are $\sigma_A^2 = 6.07 \times 10^{-2}A^2$, $\sigma_n^2 = 2.75 \times 10^{-1}$, $\sigma_E^2 = 1.38 \times 10^5$, $\sigma_{An} = -4.08 \times 10^{-18}A$, $\sigma_{En} = -1.93 \times 10^2$, and $\sigma_{AE} = -2.87 \times 10^{15}A$. The resulting 2σ precision levels of the fit lie between ±7% and ±23%, depending on temperature. Allowing ±20% for systematic errors, we estimate the accuracy of the rate coefficient measurements to vary from ±23% to ±30% at the 2σ statistical confidence limit. Figure 3 compares the present results with the experimental results of the electrical discharge studies[9−13] and with the current recommendation by Baulch et al.[20] In the earlier studies[9−13] the observed N-atom consumption rates had to be halved, as reaction 3 was followed rapidly by reaction 4. The good agreement with those $k_3(T)$ results, as well as the exponentiality of the I vs t plots, indicates that reaction 4 proceeds at a negligibly slow rate in the present work, due to the low [NO] produced.

Baulch et al.[20] give

$$k_3(300-5000\ \mathrm{K}) = 1.5 \times 10^{-14}(T/\mathrm{K}) \exp(-3270\ \mathrm{K}/T)\ \mathrm{cm}^3\ \mathrm{molecule}^{-1}\ \mathrm{s}^{-1} \quad (7)$$

Force-fitting the present data to an expression involving $T^{1.0}$, yields

$$k_3(400-1220\ \mathrm{K}) = 1.3 \times 10^{-14}(T/\mathrm{K}) \exp(-3387\ \mathrm{K}/T)\ \mathrm{cm}^3\ \mathrm{molecule}^{-1}\ \mathrm{s}^{-1} \quad (8)$$

in excellent agreement with eq 7. For eq 8, the variances and covariance are $\sigma_A^2 = 3.71 \times 10^{-2}A^2$, $\sigma_E^2 = 2.21 \times 10^4$, and $\sigma_{AE} = 28.4A$, leading to precision levels of this fit between ±5% and ±36%.

These results may be compared to information from theory. To do this, we use the transition-state theory expression

$$k_{\mathrm{TST}}(T) = \frac{k_B T}{h} \frac{Q_{\mathrm{NOO}}^{\ddagger}}{Q_{\mathrm{N}} Q_{\mathrm{O_2}}} \exp(-E_0^{\ddagger}/RT) \quad (9)$$

and assume that the vibrational and rotational motions of the transition state are separable. Here, k_B is the Boltzmann constant, *h* is the Planck constant, the *Q* are total partition functions, and $E_0^{\ddagger}$, the classical activation barrier, represents the energy change including zero-point energy going from reactants to the transition state for the reaction at 0 K.[24] The

TABLE 2: Summary of Rate Coefficient Measurements on the N + CO_2 → NO + CO Reaction

T,[a] K	P, mbar	[M], 10^{18} cm^{-3}	[N_2O],[b] 10^{15} cm^{-3}	F,[c] J	$[CO_2]_{max}$, 10^{16} cm^{-3}	z,[d] cm	$\bar{v}$, cm s^{-1}	UL,[e] 10^{-17} cm^3 molecule^{-1} s^{-1}
285	121	3.06	8.12	43	18.5	4.5	3.6	1.1
531	133	1.82	4.72	59	4.3	3.5	5.8	4.3
1064	266	0.90	2.35	118	4.0	3.5	11.4	52
1142	106	0.68	2.02	118	1.6	4.5	14.3	51

[a] $\sigma_T/T = 2\%$. [b] Photolyte. [c] Flash energy. [d] Distance from cooled inlet to reaction zone. [e] Upper limit rate coefficient.

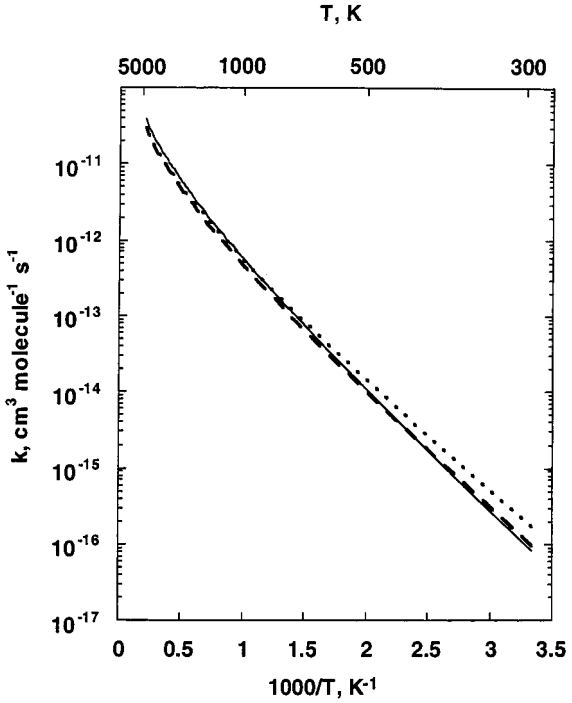

Figure 4. Comparison of TST fits using different classical activation barrier values for the N + O_2 → NO + O reaction from 300 to 5000 K: —, Baulch et al. recommendation,[20] eq 7, 300−5000 K; ···, TST fit using the Durant and Rohlfing[25] value, $E_0^{\ddagger}$= 25.9 kJ mol^{-1}; ---, TST semiempirical fit using present value, $E_0^{\ddagger}$ = 27.4 kJ mol^{-1}.

partition functions are calculated in the usual way. We use the theoretical results of Durant and Rohlfing,[25] who investigated the transition state by the G2Q method at QCISD/6-311g**, and give its geometry and vibrational frequencies. For O_2, the interatomic distance and the vibrational frequency we calculate,[26] using G94 at QCISD/6-311g**, 1.202 Å and 1662 cm^{-1}, respectively. Combining these data with their[25] value for $E_0^{\ddagger}$= 25.9 kJ mol^{-1}, and evaluating eq 9 at 100 K intervals for the 300−5000 K range, yields the dotted curve in Figure 4. It may be seen to be in good agreement with the Baulch et al. recommendation;[20] the two curves are indistinguishable above 600 K.

A fit that covers the lower temperature range better is obtained by taking $E_0^{\ddagger}$ as the only adjustable parameter of eq 9 and fitting at 100 K intervals to the experimental curve of eq 6 by minimizing the variance. The resulting semiempirical value of $E_0^{\ddagger}$ is 27.4 kJ mol^{-1}, with a root-mean-square deviation of ±8% from eq 6, slightly different from the Durant and Rohlfing value. Using this new value for $E_0^{\ddagger}$ and reevaluating eq 9 at 100 K intervals and fitting[23] yields

$$k(300-5000\ \mathrm{K}) = 9.72 \times 10^{-15}(T/\mathrm{K})^{1.01} \exp(-3121\ \mathrm{K}/T)\ \mathrm{cm}^3\ \mathrm{molecule}^{-1}\ \mathrm{s}^{-1} \quad (10)$$

This fit is shown as the dashed curve of Figure 4 and is nearly indistinguishable from the Baulch et al. recommendation[20] over the entire temperature range. The agreement between equations 6, 7, 8, and 10 shows that the present results can be accurately extrapolated over a much wider domain than the actual experimental temperature range.

N + CO_2. Over the 285−1142 K domain measured, no apparent change was observed in the pseudo-first-order rate coefficients with respect to changes in [CO_2]. The exponential decay plots observed can be attributed to N-atom diffusion from the observation zone. The upper limit rate coefficients, and the conditions under which they were obtained, are given in Table 2. The limits were calculated by multiplying the standard error of the slopes of k_{ps1} vs [CO_2] plots[21] by 2 and then dividing by the total range of [CO_2], to get the maximum possible slopes. The implicit parameters varied included P, [M], $\bar{v}$, [N_2O], and F.

The upper limit rate coefficient at 1142 K is 5×10^{-16} cm^3 molecule^{-1} s^{-1}. Extrapolating the Roth and co-workers expression[7] down to 1142 K yields 5.3×10^{-13} cm^3 molecule^{-1} s^{-1}. This value implies that if their expression is correct it cannot be extrapolated to dark zone temperatures. The present observation that k_2 is very small is in agreement with recent ab initio calculations using multireference CI and QCISD methods.[27] That work indicates a barrier for reaction 2 of at least 180 kJ mol^{-1} and a best estimate of 240 kJ mol^{-1}. One consequence of the k_2 limit values, here reported, is that when the corresponding k_1 limit is used in dark zone models, reaction 1 is found to contribute negligibly.[28]

Acknowledgment. This work has been supported by the U.S. Army under Grant DAAH04-95-1-0098. We thank Drs. W. R. Anderson and C. Chabalowski of the Army Research Laboratories for helpful discussions and making the results of unpublished work available to us, and we thank W.F. Flaherty for assistance with the experiments.

References and Notes

(1) Vanderhoff, J. A.; Anderson, W. R.; Kotlar, A. J. 29th JANAF Combustion Meeting, 1992.
(2) Chase, M. W.; Davies, C. A.; Downey, J. R., Jr.; Frurip, D. J.; McDonald, R. A.; Syverud, A. N. JANAF Thermochemical Tables. *J. Phys. Chem. Ref. Data* **1985**, *14*, Suppl. 1.
(3) Avramenko, L. I.; Krasnen'kov, V. M. *Bull. Acad. Sci. USSR, Div. Chem. Sci.* **1967**, 501.
(4) Rawlins, W. T.; Kaufman, F. *J. Chem. Phys.* **1976**, *64*, 1128.
(5) Campbell, I. M.; Thrush, B. A. *Trans. Faraday Soc.* **1966**, *62*, 3366.
(6) Herron, J. T.; Huie, R. E. *J. Phys. Chem.* **1968**, *72*, 2235.
(7) Lindackers, D.; Burmeister, M.; Roth, P. *Combust. Flame* **1990**, *81*, 251.
(8) Jones, J. C. *Combustion Science, Principles and Practice*; Millenium Books: Newtown, Australia, 1993; p 108.
(9) Becker, K. H.; Groth, W.; Kley, D. *Z. Naturforsch.* **1969**, *24A*, 1280.
(10) Baulch, D. L.; Drysdale, D. D.; Horne, D. G. *Evaluated Kinetic Data for High Temperature Reactions, Vol. 2, Homogeneous Gas Phase Reactions of the $H_2/N_2/O_2$ System*; Butterworth: London, 1973; p 193.
(11) Wilson, W. E. *J. Chem. Phys.* **1967**, *46*, 2017.
(12) Vlastaras, A. S.; Winkler, C. A. *Can. J. Chem.* **1967**, *45*, 2837.
(13) Clyne, M. A. A.; Thrush, B. A. *Proc. R. Soc. London A* **1961**, *261*, 259.
(14) Ko, T.; Marshall, P.; Fontijn, A. *J. Phys. Chem.* **1990**, *94*, 1401.
(15) Okabe, H. *Photochemistry of Small Molecules*; Wiley-Interscience: New York, 1978; p 219 ff.

(16) Mahmud, K.; Marshall, P.; Fontijn, A. *J. Phys. Chem.* **1987**, *91*, 1568.
(17) Husain, D.; Slater, K. H. *J. Chem. Soc., Faraday Trans. 2* **1980**, 76, 606.
(18) Hranisavljevic, J.; Fontijn, A. *J. Phys. Chem.* **1995**, *99*, 12809.
(19) Lee, J. H.; Michael, J. V.; Payne, W. A.; Stief, L. J. *J. Chem. Phys.* **1978**, *69*, 3069.
(20) Baulch, D. L.; Cobos, C. J.; Cox, R. A.; Frank, P.; Hayman, G.; Just, Th.; Kerr, J. A.; Murrells, T.; Pilling, M. J.; Troe, J.; Walker, R. W.; Warnatz, J. *J. Phys. Chem. Ref. Data* **1994**, *23*, 847; *Combust. Flame* **1994**, *98*, 59.
(21) Marshall, P. *Comput. Chem.* **1987**, *11*, 219.
(22) Ko, T.; Adusei, G. Y.; Fontijn, A. *J. Phys. Chem.* **1991**, *95*, 8745.
(23) Bevington, P. R. *Data Reduction and Error Analysis for the Physical Sciences*; McGraw-Hill: New York, 1969; Chapter 4.
(24) Johnston, H. S. *Gas Phase Reaction Rate Theory*; Ronald: New York, 1966; Chapter 9.
(25) Durant, J. L.; Rohlfing, C. M. *J. Chem. Phys.* **1993**, *98*, 8031.
(26) Frisch, M. J.; Trucks, G. W.; Schlegel, H. B.; Gill, P. M. W.; Johnson, B. G.; Robb, M. A.; Cheeseman, J. R.; Keith, T. A.; Petersson, G. A.; Montgomery, J. A.; Raghavachari, K.; Al-Laham, M. A.; Zakrzewski, V. G.; Ortiz, J. V.; Foresman, J. B.; Cioslowski, J.; Stefanov, B. B.; Nanayakkara, A.; Challacombe, M.; Peng, C. Y.; Ayala, P. Y.; Chen, W.; Wong, M. W.; Andres, J. L.; Replogle, E. S.; Gomperts, R.; Martin, R. L.; Fox, D. J.; Binkley, J. S.; Defrees, D. J.; Baker, J.; Stewart, J. P.; Head-Gordon, M.; Gonzalez, C.; Pople, J. A. *Gaussian 94* (Revision C.3); Gaussian, Inc.: Pittsburgh, PA, 1995.
(27) Chabalowski, C.; Manaa, M. R. Private communication to the authors, 1997.
(28) Anderson, W. R. Private communication to the authors, 1997.